

Synthesis and Reactivity of Dinuclear Platinum Complexes. NMR Spectra of $[\text{Pt}_2(\text{PMe}_3)_6][\text{hfac}]_2$ and an Unusual β -Diketonate Bridging Mode in $[\text{Pt}_2(\mu\text{-hfac})(\text{PMe}_3)_4][\text{hfac}]$

Wenbin Lin, Scott R. Wilson, and Gregory S. Girolami*

School of Chemical Sciences, University of Illinois at Urbana-Champaign, 601 South Goodwin Avenue, Urbana, Illinois 61801

Received August 8, 1996[⊗]

Comproportionation of the platinum(0) complex $\text{Pt}(\text{PMe}_3)_4$ with the platinum(II) hexafluoroacetylacetonate complexes $\text{Pt}(\text{hfac})_2$ or $[\text{Pt}(\text{hfac})(\text{PMe}_3)_2][\text{hfac}]$ yields diplatinum species of stoichiometry $[\text{Pt}_2(\mu\text{-hfac})(\text{PMe}_3)_4][\text{hfac}]$, **1**, and $[\text{Pt}_2(\text{PMe}_3)_6][\text{hfac}]_2$, **2**, respectively. The NMR spectra and X-ray crystal structure of **1** show that the two platinum centers are chemically inequivalent; one is a square-planar platinum(II) center, and the other is trigonal planar platinum(0) center. One of the hfac groups is anionic while the other bridges between the two platinum atoms. Each platinum center bears two PMe_3 ligands, and the bridging hfac group is bound to one platinum center in the usual fashion through its two oxygen atoms. The bridging hfac group, however, is bound to the other platinum center as an η^2 alkene ligand via its methine carbon and one of the two carbonyl carbons. The two platinum atoms do not interact directly with one another and are separated by 3.786(1) Å. The ^1H NMR spectra of the hexakis(trimethylphosphine)diplatinum complex **2** are consistent with a structure in which the two platinum centers are connected by a Pt–Pt bond and the six PMe_3 groups complete two mutually perpendicular square-planar coordination environments. Treatment of $\text{Pt}(\text{PMe}_3)_4$ with $[\text{Pt}(\text{PMe}_3)_4][\text{hfac}]_2$ in tetrahydrofuran gives the platinum(II) hydride $[\text{PtH}(\text{PMe}_3)_4][\text{hfac}]$, **3**. The ^1H and $^{31}\text{P}\{^1\text{H}\}$ NMR data of **3** are consistent with a trigonal bipyramidal structure; the hydride ligand occupies an axial position. The hydride ligand evidently arises from adventitious water. Thermolysis of **1** and **2** under vacuum gives the platinum(II) methyl complex $[\text{PtMe}(\text{PMe}_3)_3][\text{hfac}]$ as a result of the cleavage of one of the P–C bonds in the PMe_3 ligands. Crystal data for **1** at -75°C : triclinic, space group $P\bar{1}$, $a = 9.848(2)$ Å, $b = 12.079(3)$ Å, $c = 15.373(3)$ Å, $\alpha = 84.70(2)^\circ$, $\beta = 78.57(2)^\circ$, $\gamma = 80.30(2)^\circ$, $V = 1763(7)$ Å³, $Z = 2$, $R_F = 0.043$, $R_{wF} = 0.044$ for 400 variables and 3360 reflections with $I > 2.58 \sigma(I)$.

Introduction

The fabrication of metal and ceramic thin films by metal–organic chemical vapor deposition (MOCVD) has been an area of active research in the past few years.^{1–5} The chemical vapor deposition of platinum group metals is of particular interest, because these metals have many potential uses as interconnects and contacts in microelectronic devices.^{6–11} We have previously described the preparation and reactivity of the palladium(I) complex $[\text{Pd}_2(\text{PMe}_3)_6][\text{hfac}]_2$ and an assessment of its potential

as a source for the deposition of palladium films by CVD.¹² Our interest in this dinuclear phosphine complex arose from an effort to develop and study new MOCVD methods that involve redox processes, in this case the disproportionation of Pd^{I} to Pd^{II} and Pd^0 .¹² We have extended our studies by investigating the preparation and reactivity of corresponding platinum(I) complexes. We now describe the synthesis and characterization of the novel dinuclear platinum complexes $[\text{Pt}_2(\mu\text{-hfac})(\text{PMe}_3)_4][\text{hfac}]$, **1**, and $[\text{Pt}_2(\text{PMe}_3)_6][\text{hfac}]_2$, **2**, and the platinum(II) hydride $[\text{PtH}(\text{PMe}_3)_4][\text{hfac}]$, **3**. The suitabilities of these complexes to serve as MOCVD precursors have been investigated; of interest in this context is their ability to activate the phosphorus–carbon bonds of the PMe_3 ligands.

Results and Discussion

Before the synthesis and characterization of the new dinuclear platinum complexes are described, the preparation of several platinum(0) and platinum(II) starting materials will be discussed.

Synthesis of Tetrakis(trimethylphosphine)platinum(0), $\text{Pt}(\text{PMe}_3)_4$. The procedure employed for the synthesis of $\text{Pt}(\text{PMe}_3)_4$ is based on one of the recipes used to synthesize tetrakis(triethylphosphine)platinum(0), $\text{Pt}(\text{PET}_3)_4$.¹³ Tetrakis(trimethylphosphine)platinum(0) is prepared by stirring a mixture of K_2PtCl_4 , PMe_3 , and KOH in ethanol/water at 60°C for 3 h. This procedure gives $\text{Pt}(\text{PMe}_3)_4$ in about 40% yield, which is

- [⊗] Abstract published in *Advance ACS Abstracts*, May 15, 1997.
- (1) Kudas, T. T.; Hampden-Smith, M. J. *The Chemistry of Metal CVD*; VCH Publishers: New York, 1994.
 - (2) Spencer, J. T. *Prog. Inorg. Chem.* **1994**, *41*, 145–237.
 - (3) Girolami, G. S.; Gozum, J. E. *Mater. Res. Soc. Symp. Proc.* **1990**, *168*, 319–329.
 - (4) *Chemical Vapor Deposition of Refractory Metals and Ceramics*; Besman, T. M., Gallois, B. M., Eds.; Materials Research Society: Pittsburgh, PA, 1990. *Chemical Vapor Deposition of Refractory Metals and Ceramics II*; Besman, T. M., Gallois, B. M., Warren, J. W., Eds.; Materials Research Society: Pittsburgh, PA, 1992.
 - (5) Jensen, K. F.; Kern, W. In *Thin Film Processes II*; Vossen, J. L., Kern, W., Eds.; Academic: Boston, MA, 1991; Chapter III-1.
 - (6) Lin, W.; Warren, T. H.; Nuzzo, R. G.; Girolami, G. S. *J. Am. Chem. Soc.* **1993**, *115*, 11644–11645.
 - (7) Lin, W.; Nuzzo, R. G.; Girolami, G. S. *J. Am. Chem. Soc.* **1996**, *118*, 5988–5996.
 - (8) Lin, W.; Wiegand, B. C.; Nuzzo, R. G.; Girolami, G. S. *J. Am. Chem. Soc.* **1996**, *118*, 5977–5987.
 - (9) Xue, Z. L.; Thrindandam, H.; Kaesz, H. D.; Hicks, R. F. *Chem. Mater.* **1992**, *4*, 162–166.
 - (10) Yuan, Z.; Jiang, D.; Naftel, S. J.; Sham, T.-K.; Puddephatt, R. J. *Chem. Mater.* **1994**, *6*, 2151–2158.
 - (11) Kubiak, C. P.; Broeker, G. K.; Granger, R. M.; Lemke, F. R.; Morgenstern, D. A. *Adv. Chem. Ser.* **1993**, *238*, 165–184.

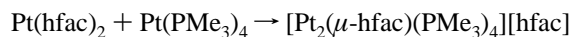
- (12) Lin, W.; Wilson, S. R.; Girolami, G. S. *Inorg. Chem.* **1994**, *33*, 2265–2272.
- (13) Yoshida, T.; Matsuda, T.; Otsuka, S. *Inorg. Synth.* **1979**, *19*, 110–111.

an improvement over the literature methods for the preparation of $\text{Pt}(\text{PMe}_3)_4$.^{14,15} The product has been characterized by ^1H and $^{31}\text{P}\{^1\text{H}\}$ NMR spectroscopy (see Experimental Section).

Synthesis and Characterization of Trimethylphosphine Adducts of Platinum(II) Hexafluoroacetylacetonate: $[\text{Pt}(\text{hfac})(\text{PMe}_3)_2][\text{hfac}]$ and $[\text{Pt}(\text{PMe}_3)_4][\text{hfac}]_2$. The bis(trimethylphosphine) adduct $[\text{Pt}(\text{hfac})(\text{PMe}_3)_2][\text{hfac}]$ is prepared by treatment of $\text{Pt}(\text{hfac})_2$ with 2 equiv of PMe_3 in diethyl ether. The presence of two $\text{C}=\text{O}$ stretches in its infrared spectrum clearly indicates that there are two hfac environments: The peak at 1673 cm^{-1} is due to an ionic hfac group, while the peak at 1637 cm^{-1} is assignable to a coordinated hfac group. The ionic nature of $[\text{Pt}(\text{hfac})(\text{PMe}_3)_2][\text{hfac}]$ is further supported by its electrical conductivity of $30.0\ \Omega^{-1}\text{ cm}^2\text{ mol}^{-1}$ in nitrobenzene, which is in the $20\text{--}30\ \Omega^{-1}\text{ cm}^2\text{ mol}^{-1}$ range for 1:1 electrolytes in this solvent.¹⁶ Undoubtedly, the platinum center in $[\text{Pt}(\text{hfac})(\text{PMe}_3)_2][\text{hfac}]$ adopts a square-planar structure and is bound to the oxygen atoms of the coordinated hfac group and to two PMe_3 groups. This complex is similar to other 2:1 Lewis base adducts of $\text{Pt}(\text{hfac})_2$ that have been described.^{17,18} The ^1H NMR spectrum of $[\text{Pt}(\text{hfac})(\text{PMe}_3)_2][\text{hfac}]$ shows a doublet at δ 1.85 and a broad singlet at δ 5.95 for the PMe_3 and hfac protons, respectively. The presence of only a single hfac methine resonance in the ^1H NMR spectrum demonstrates that the ionic and coordinated hfac groups rapidly exchange in solution at $25\text{ }^\circ\text{C}$.^{17,18}

When $\text{Pt}(\text{hfac})_2$ is treated with 4 equiv of PMe_3 in diethyl ether, a white precipitate forms immediately. Elemental analyses and IR and NMR spectroscopy show that the white precipitate is an hfac salt of the tetrakis(trimethylphosphine)-platinum(II) dication, $[\text{Pt}(\text{PMe}_3)_4][\text{hfac}]_2$. The platinum center probably adopts a square-planar geometry like other known 4:1 Lewis base adducts of $\text{Pt}(\text{hfac})_2$.^{17,18}

Synthesis and Characterization of $[\text{Pt}_2(\mu\text{-hfac})(\text{PMe}_3)_4][\text{hfac}]$, **1.** Comproportionation of platinum(II) hexafluoroacetylacetonate $\text{Pt}(\text{hfac})_2$ and the platinum(0) trimethylphosphine complex $\text{Pt}(\text{PMe}_3)_4$, a reaction in which there are a total of 2 equiv of PMe_3 per metal center, yields a red precipitate which can be recrystallized from a mixture of dichloromethane and diethyl ether to afford orange crystals. Although the empirical formula of the product is " $\text{Pt}(\text{hfac})(\text{PMe}_3)_2$ ", the diamagnetism of this material indicates that it is not monomeric. Instead, we will show that this product is best formulated as $[\text{Pt}_2(\mu\text{-hfac})(\text{PMe}_3)_4][\text{hfac}]$, **1**.

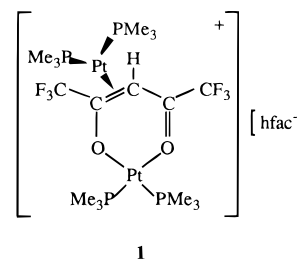


1

The ^1H NMR spectrum of **1** (Supporting Information) shows two equal-intensity resonances for two different types of hfac groups: a singlet at δ 6.28 and a broad peak at δ 4.29, the latter of which shows coupling to ^{195}Pt ($^2J_{\text{PtH}} = 39\text{ Hz}$). The singlet at δ 6.28 can be assigned to a noncoordinating, anionic hfac group, while the signal at δ 4.29 is due to a coordinated hfac group. The coupling of the methine proton to the ^{195}Pt nucleus suggests that the hfac group is bound to a platinum center through its methine carbon. This two-bond platinum-proton coupling constant, however, is considerably smaller than

those of acetylacetonato groups σ -bound to platinum centers through their methine carbons; these coupling constants are normally 120 Hz .^{19,20} The 39 Hz coupling constant is, in fact, much closer to the value observed for platinum-alkene complexes.²¹ This comparison suggests that the hfac group is bound to one platinum center through its methine and carbonyl carbons. Such a binding mode has been proposed for the coordinated acetylacetonate ligand in the platinum(II) complex $\text{Pt}(\text{acac})(\text{acacH})\text{Cl}$,²² but no X-ray single-crystal structure determination has been carried out on this molecule.

The ^1H NMR spectrum of **1** contains two sets of pseudo-triplets at δ 1.22 and 1.18 for the protons of the PMe_3 groups. The presence of the two different PMe_3 environments is further manifested in the $^{31}\text{P}\{^1\text{H}\}$ NMR spectrum of **1**, which shows two equal-intensity resonances at δ -22.3 and -27.0 . There is no coupling between these two PMe_3 environments, which strongly suggests that there is no direct Pt-Pt bonding between the platinum centers in **1**. A solution electrical conductivity measurement shows that **1** is a 1:1 electrolyte in methanol. We will show below that the bound hfac group exists in its enolic form and bridges between the two platinum centers. It is bound to one platinum center through its two oxygens and to the other through its olefinic carbons:



1

The IR spectrum of **1** is consistent with this structure. Although there is no readily identifiable band for the coordinated hfac group, there is a single ν_{CO} band at 1670 cm^{-1} for the anionic hfac group.^{12,23-25} A hfac group σ -bound to a metal center through its methine carbon gives an IR stretch above 1700 cm^{-1} ,²⁶ but for **1** the carbonyl stretch of the bridging hfac group in its enolic form should appear at somewhat lower frequency and may be obscured by the carbonyl stretch of the anionic hfac group.

X-ray Crystal Structure of $[\text{Pt}_2(\mu\text{-hfac})(\text{PMe}_3)_4][\text{hfac}]$, **1.** An X-ray single-crystal structure determination of **1** has been carried out in order to confirm its structure and to obtain the structural parameters characteristic of this new hfac bonding mode. Single crystals of **1**, grown from tetrahydrofuran, crystallize in the triclinic space group $P\bar{1}$ with two molecules in the unit cell. There is no crystallographic symmetry imposed on either of the two molecules, but they are related by the inversion center. Crystal data are presented in Table 1, and selected bond distances and angles are given in Table 2.

Figure 1 shows an ORTEP drawing of the $[\text{Pt}_2(\mu\text{-hfac})(\text{PMe}_3)_4]^+$ cation. Consistent with the spectroscopic data,

- (14) Mann, B. E.; Musco, A. *J. Chem. Soc., Dalton Trans.* **1980**, 776-785.
 (15) Edwards, H. G. M. *Spectrochim. Acta, Part A* **1986**, *42*, 1401-1404.
 (16) Geary, W. J. *Coord. Chem. Rev.* **1972**, *7*, 81-122.
 (17) Okeya, S.; Nakamura, Y.; Kawaguchi, S. *Bull. Chem. Soc. Jpn.* **1981**, *54*, 3396-3408.
 (18) Okeya, S.; Nakamura, Y.; Kawaguchi, S. *Bull. Chem. Soc. Jpn.* **1982**, *55*, 1460-1466.

- (19) Lewis, J.; Long, R. F.; Oldham, C. *J. Chem. Soc.* **1965**, 6740-6747.
 (20) Gibson, D.; Lewis, J.; Oldham, C. *J. Chem. Soc. A* **1966**, 1453-1456.
 (21) Nuzzo, R. G.; McCarthy, T. J.; Whitesides, G. M. *Inorg. Chem.* **1981**, *20*, 1312-1314.
 (22) Allen, G.; Lewis, J.; Long, R. F.; Oldham, C. *Nature* **1964**, *202*, 589-590.
 (23) Siedle, A. R.; Newmark, R. A.; Kruger, A. A.; Pignolet, L. H. *Inorg. Chem.* **1981**, *20*, 3399-3404.
 (24) Chi, K. M.; Farkas, J.; Hampden-Smith, M. J.; Kodas, T. T.; Duesler, E. N. *J. Chem. Soc., Dalton Trans.* **1992**, 3111-3117.
 (25) Siedle, A. R.; Newmark, R. A.; Pignolet, L. H. *J. Am. Chem. Soc.* **1982**, *104*, 6584-6590.
 (26) Hartman, F. A.; Kilner, M.; Wojcicki, A. *Inorg. Chem.* **1967**, *6*, 34-40.

Table 1. Crystal Data for $[\text{Pt}_2(\mu\text{-hfac})(\text{PMe}_3)_4][\text{hfac}]$, **1**

$\text{C}_{22}\text{H}_{38}\text{P}_4\text{F}_{12}\text{O}_4\text{Pt}_2$	space gp: $P\bar{1}$
$a = 9.848(2) \text{ \AA}$	$T = -75 \text{ }^\circ\text{C}$
$b = 12.079(3) \text{ \AA}$	$\lambda = 0.71073 \text{ \AA}$
$c = 15.373(3) \text{ \AA}$	mol wt = 1108.60
$\alpha = 84.70(2)^\circ$	$\rho_{\text{calcd}} = 2.088 \text{ g cm}^{-3}$
$\beta = 78.57(2)^\circ$	$\mu_{\text{calcd}} = 82.75 \text{ cm}^{-1}$
$\gamma = 80.30(2)^\circ$	transm coeff = 0.398–0.629
$V = 1763(7) \text{ \AA}^3$	$R_F = 0.043^a$
$Z = 2$	$R_{wF} = 0.044^b$

$$^a R_F = \sum(|F_o| - |F_c|)/\sum|F_o|. \quad ^b R_{wF} = \{\sum w(|F_o| - |F_c|)^2/\sum|F_o|^2\}^{1/2}.$$

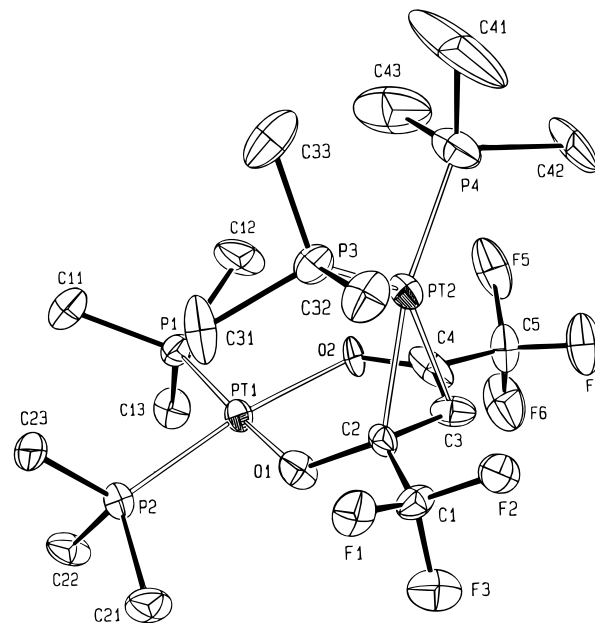
Table 2. Selected Bond Distances and Angles for $[\text{Pt}_2(\mu\text{-hfac})(\text{PMe}_3)_4][\text{hfac}]$, **1**

Bond Distances (\AA)			
Pt(1)–P(1)	2.223(4)	C(3)–C(4)	1.37(2)
Pt(1)–P(2)	2.218(4)	C(4)–O(2)	1.31(2)
Pt(2)–P(3)	2.241(4)	C(1)–C(2)	1.48(2)
Pt(2)–P(4)	2.301(5)	C(4)–C(5)	1.51(2)
Pt(1)–O(1)	2.023(9)	C(9)–O(4)	1.28(2)
Pt(1)–O(2)	2.050(9)	C(7)–O(3)	1.23(2)
Pt(2)–C(2)	2.18(1)	C(6)–C(7)	1.48(3)
Pt(2)–C(3)	2.17(1)	C(7)–C(8)	1.38(3)
C(2)–O(1)	1.36(2)	C(8)–C(9)	1.42(3)
C(2)–C(3)	1.43(2)	C(9)–C(10)	1.45(4)

Bond Angles (deg)			
P(1)–Pt(1)–P(2)	95.5(1)	Pt(2)–C(3)–C(2)	71.1(8)
P(1)–Pt(1)–O(1)	175.2(3)	Pt(2)–C(3)–C(4)	89(1)
P(1)–Pt(1)–O(2)	87.4(3)	Pt(2)–C(2)–C(1)	117(1)
P(2)–Pt(1)–O(1)	86.3(3)	O(1)–C(2)–C(1)	109(1)
P(2)–Pt(1)–O(2)	171.7(3)	O(1)–C(2)–C(3)	124(1)
O(1)–Pt(1)–O(2)	91.4(4)	C(1)–C(2)–C(3)	115(1)
P(3)–Pt(2)–P(4)	104.2(2)	C(2)–C(3)–C(4)	121(1)
P(3)–Pt(2)–C(2)	97.3(4)	O(2)–C(4)–C(3)	129(1)
P(3)–Pt(2)–C(3)	91.4(4)	O(2)–C(4)–C(5)	112(1)
P(4)–Pt(2)–C(2)	158.2(4)	C(3)–C(4)–C(5)	117(2)
P(4)–Pt(2)–C(3)	120.4(4)	O(3)–C(7)–C(6)	115(2)
C(2)–Pt(2)–C(3)	135.2(4)	O(3)–C(7)–C(8)	127(2)
Pt(1)–O(1)–C(2)	122.0(8)	C(6)–C(7)–C(8)	118(2)
Pt(1)–O(2)–C(4)	123.7(9)	C(7)–C(8)–C(9)	128(2)
Pt(2)–C(2)–C(1)	117(1)	O(4)–C(9)–C(8)	122(2)
Pt(2)–C(2)–C(3)	70.4(8)	O(4)–C(9)–C(10)	117(2)
Pt(2)–C(2)–O(1)	118.4(9)	C(8)–C(9)–C(10)	121(2)

compound **1** contains two platinum centers bridged by a hfac group. The coordinated hfac group is bound to one platinum center through its two oxygen atoms and to the other platinum center through its methine and carbonyl carbons. The other hfac group serves as a counterion. Each platinum center is also coordinated to two PMe_3 ligands and adopts a square planar or trigonal planar geometry. There is no direct bonding between the Pt(1) and Pt(2) atoms; the Pt(1)–Pt(2) distance is 3.786(1) \AA . To the best of our knowledge, this is the first well-established example of an acetylacetonato group bound to transition metals through its olefinic carbons in its enolic form. A few other examples of β -diketonate ligands that bridge between two metals are known, but the bridging modes are very different from that in **1**.^{27,28}

Pt(1) and the four directly attached atoms are almost coplanar, and the distances of these atoms from the least-squares plane are 0.025, 0.101, –0.115, 0.116, and –0.127 \AA for Pt(1), P(1), P(2), O(1), and O(2), respectively. The Pt(1)–O(1) and Pt(1)–O(2) distances of 2.023(9) and 2.050(9) \AA , respectively, are shorter than the Pt–O distances reported for other platinum(II) acetylacetonate complexes.^{29,30} The coordination of the hfac

**Figure 1.** ORTEP diagram of the $[\text{Pt}_2(\mu\text{-hfac})(\text{PMe}_3)_4]^+$ cation in **1**. The ellipsoids represent the 35% probability density surfaces.

group to the Pt(1) center through its two oxygen atoms lengthens the C–O distances, as expected. The average C–O distance in the coordinated hfac group is 1.34 \AA while the average C–O distance in the anionic hfac group is 1.26 \AA . The Pt(1)–P(1) and Pt(1)–P(2) distances (which average 2.22 \AA) are well within the 2.13–2.32 \AA range observed for Pt–P bonds in other known platinum(II) trimethylphosphine complexes.^{31–33}

Pt(2) and its four coordinating atoms are also almost coplanar, as shown by the out-of-plane distances of –0.005, 0.047, –0.036, –0.108, and 0.101 \AA for Pt(2), P(3), P(4), C(2), and C(3), respectively. The two square planes about Pt(1) and Pt(2) are essentially orthogonal and describe a dihedral angle of 87.8°. Undoubtedly, compound **1** adopts this arrangement in order to maximize the bonding to the bridging hfac group and to minimize steric repulsions. The Pt(2)–P(3) and Pt(2)–P(4) distances (which average 2.27 \AA) are slightly longer than those to Pt(1).

A useful indicator of the binding mode of platinum olefin complexes is the dihedral angle between the plane defined by Pt and the two olefinic carbons and the plane defined by Pt and the other directly-bonded atoms.³⁴ For zerovalent platinum complexes of the type $\text{Pt}(\text{alkene})(\text{PR}_3)_2$ (where R is an alkyl, aryl, or halo group), this dihedral angle is near zero; in contrast, for platinum(II) olefin complexes such as Zeise's salt, this value is close to 90°. The corresponding dihedral angle defined by the atoms bonded to Pt(2) is about 8°. This is within the range observed for other $\text{Pt}(\text{alkene})(\text{PR}_3)_2$ complexes.³⁴ Therefore, compound **1** should be viewed as a mixed-valence diplatinum complex: Pt(1) is in the +2 oxidation state while Pt(2) is zerovalent.

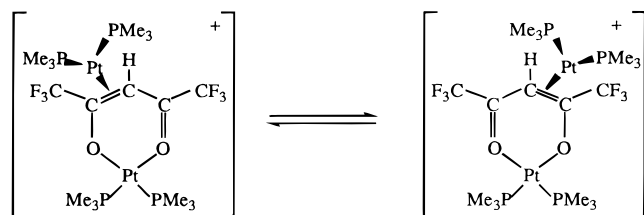
(29) Swallow, A. G.; Truter, M. R. *Proc. R. Soc.* **1960**, 254A, 205–217.(30) Yamaguchi, T.; Sasaki, Y.; Ito, T. *J. Am. Chem. Soc.* **1990**, 112, 4038–4040.(31) Packett, D. L.; Syed, A.; Troglor, W. C. *Organometallics* **1988**, 7, 159–166.(32) Ogawa, H.; Onitsuka, K.; Joh, T.; Takahashi, S. *Organometallics* **1988**, 7, 2257–2260.(33) Osakada, K.; Kim, Y.-J.; Yamamoto, A. *J. Organomet. Chem.* **1990**, 382, 303–317.(34) Hartley, F. R. In *Comprehensive Organometallic Chemistry*; Wilkinson, G., Stone, F. G. A., Abel, E. W., Eds.; Pergamon Press: New York, 1982; Vol. 6, Chapter 39.(27) Alvarez, B.; Bois, C.; Jeanmin, Y.; Miguel, D.; Riera, V. *Inorg. Chem.* **1993**, 32, 3783–3785.(28) Bailey, A.; Corbitt, T. S.; Hampden-Smith, M. J.; Duesler, E. N.; Kodas, T. T. *Polyhedron* **1993**, 12, 1785–1792.

As a result of its coordination to Pt(2), the C(2)–C(3) bond (1.43 Å) is longer than the C(3)–C(4) bond (1.37 Å). The C(2)–Pt(2)–C(3) angle of 38.5(5) Å is slightly smaller than the 40–43° values observed in other known zerovalent platinum alkene complexes.³⁴ In other Pt(alkene)(PR₃)₂ species, there is often an inverse correlation between the length of the Pt–C bond and the length of the trans Pt–P bond.³⁴ In **1**, the two Pt(2)–C bond distances are equal within experimental error (2.18(1) Å) but the Pt(2)–P(3) and Pt(2)–P(4) bonds of 2.301(5) and 2.241(4) Å, respectively, are significantly different.

The anionic hfac group adopts a U-shaped structure very similar to that found previously in several other hfac salts.^{12,23,24} The C₅O₂ skeleton of the hfac anion is essentially planar: The C–C–C–C and C–C–C–O torsion angles are all very near 0 or 180°, and the largest deviation of the five carbon and two oxygen atoms from the mean plane is only 0.026 Å. The two C–O distances of 1.23(2) and 1.28(2) Å and the two C–C distances to the methine carbon of 1.38(3) and 1.42(3) Å show that the hfac anion is symmetrical and that its π-system is delocalized.

Dynamic Exchange Process in [Pt₂(μ-hfac)(PMe₃)₄][hfac], **1**.

The X-ray single-crystal structure determination shows that **1** is an unsymmetric molecule in the solid state and that there are four different PMe₃ environments. In contrast, the room-temperature ³¹P{¹H} NMR spectrum of **1** only shows two PMe₃ environments, so that there must be a dynamic process which makes the PMe₃ groups on each platinum center equivalent. In fact, the resonance at δ –22.3 (which is probably due to the PMe₃ groups on the Pt(2) atom) in the room temperature ³¹P{¹H} NMR spectrum of **1** is rather broad. As the temperature is lowered, this resonance becomes even broader, but we have not been able to freeze out this dynamic process even at –90 °C. On the other hand, the resonance at δ –27.0 is rather sharp throughout the temperature range studied; evidently the chemical shift difference between the two PMe₃ groups on the Pt(1) center is smaller. Because rotation of the alkene group is a high-energy process in other zerovalent platinum complexes of the type Pt(alkene)(PR₃)₂,³⁴ rotation of the C(2)–C(3) group around its bond to the Pt(2) center is unlikely to be the dynamic exchange process that **1** undergoes; furthermore, such a mechanism would not exchange the PMe₃ groups on Pt(1). The only reasonable mechanism for this dynamic process is the hopping of the Pt(2) atom between the C(2)–C(3) and C(3)–C(4) bonds. Such a hopping process would make the PMe₃ groups on each platinum center equivalent.



Interestingly, the ¹⁹⁵Pt satellite peaks for the resonance at δ –27.0 become broad at low temperatures. We do not think that this is a result of slowing of the hopping process because the central peak at δ –27.0 remains sharp at these temperatures. Instead, we believe that the broadening of the ¹⁹⁵Pt satellite peaks arises from relaxation of the ¹⁹⁵Pt nuclei via chemical shift anisotropy effects.³⁵

Synthesis and Characterization of [Pt₂(PMe₃)₆][hfac]₂, **2**.

The comproportionation reaction between equal molar amounts

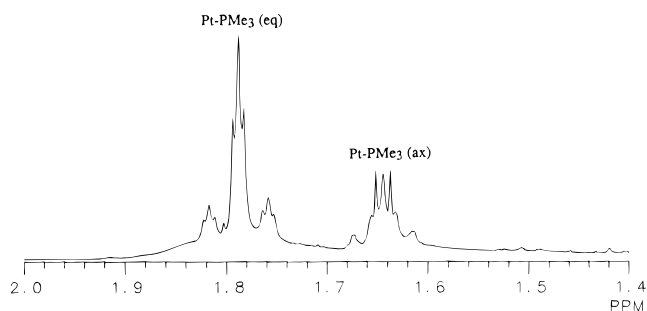
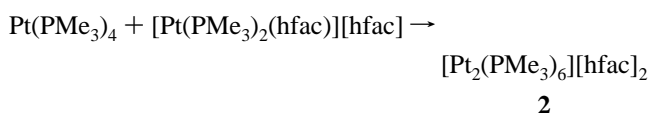
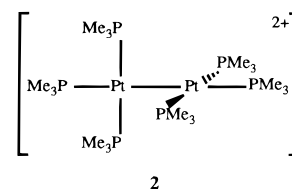


Figure 2. 500 MHz ¹H NMR spectrum of [Pt₂(PMe₃)₆][hfac]₂, **2**, in CD₂Cl₂ at 25 °C.

of Pt(PMe₃)₄ and [Pt(PMe₃)₂(hfac)][hfac], a reaction in which there are a total of 3 equiv of PMe₃ per metal center, yields a product different from that described in the preceding section. This preparation is similar to that of [Pd₂(PMe₃)₆][hfac]₂,¹² and we will show below that the product, [Pt₂(PMe₃)₆][hfac]₂, **2**, has a structure similar to that of its palladium analogue.



The dimeric nature of **2** can be inferred from its diamagnetism and its electrical conductivity in methanol, which corresponds to that of a 2:1 electrolyte. The ¹H NMR spectrum of **2** shows two PMe₃ resonances: a pseudotriplet at δ 1.79 (²J_{H–P} + ⁴J_{H–P} = 5.5 Hz, ²J_{Pt–H} = 29.5 Hz) and a multiplet at δ 1.18 (²J_{Pt–H} = 29.0 Hz) with relative intensities of 2:1 (Figure 2). The proton resonance for the anionic hfac groups appears as a singlet at δ 5.45. These spectroscopic data are very similar to those of [Pd₂(PMe₃)₆][hfac]₂.¹² In view of the known crystal structures of the palladium complexes [Pd₂(PMe₃)₆]²⁺¹² and [Pd₂(CNMe)₆]²⁺,³⁶ we conclude that **2** has a similar dimeric structure



in which the two platinum centers are connected by a Pt–Pt bond and the six PMe₃ groups occupy the terminal sites of two mutually perpendicular square-planar environments. The ³¹P{¹H} NMR spectrum of **2** is rather complex because three ¹⁹⁵Pt isotopologues are present that correspond to the spin systems AA'B₂B'₂, ABC₂D₂M, and AA'B₂B'₂MM', depending on how many ¹⁹⁵Pt nuclei are present. We have successfully simulated the ³¹P{¹H} NMR spectrum of **2** with a statistical distribution of these three spin systems based on the natural abundance of ¹⁹⁵Pt (33.7%) (Figure 3). The three-bond phosphorus–phosphorus coupling constant between the two axial PMe₃ groups (i.e., through the Pt–Pt bond) is 161 Hz. For comparison, the corresponding coupling constant is approximately 80 Hz in the dipalladium complex [Pd₂(PMe₃)₆][hfac]₂ and 185 Hz in the mixed-metal complex [PdPt(PMe₃)₆][hfac]₂.¹² The ¹J_{Pt–P}, ²J_{Pt–P}, and ²J_{PP} coupling constants (see Experimental Section) are similar to those reported for other dinuclear platinum(I) phosphine complexes.^{37,38} The ¹J_{Pt–Pt} coupling

(36) Goldberg, S. Z.; Eisenberg, R. *Inorg. Chem.* **1976**, *15*, 535–541.

(35) Ismail, I. M.; Kerrison, S. J. S.; Sadler, P. J. *Polyhedron* **1982**, *1*, 57–59.

(37) Krevor, J. V. Z.; Simonis, U.; Karson, A.; Castro, C.; Aliakbar, M. *Inorg. Chem.* **1992**, *31*, 312–317.

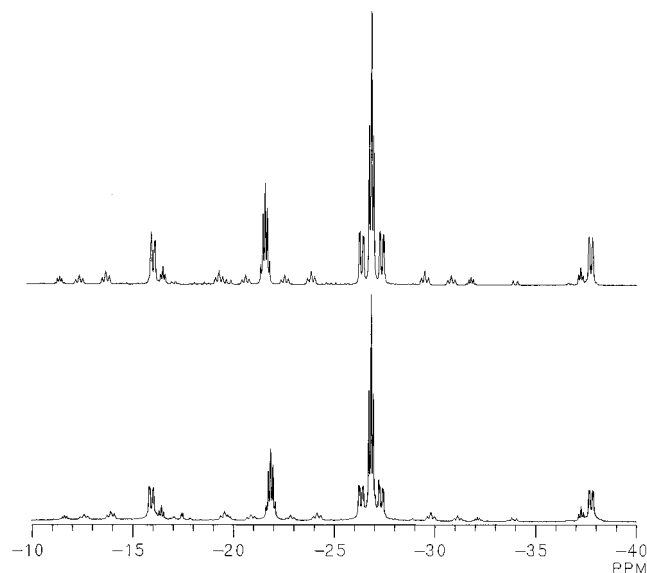
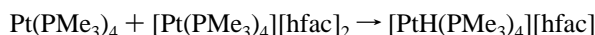


Figure 3. Bottom: 121.64 MHz $^{31}\text{P}\{^1\text{H}\}$ NMR spectrum of $[\text{Pt}_2(\text{PMe}_3)_6][\text{hfac}]_2$, **2**, in CD_2Cl_2 at 25 °C. Top: Simulated spectrum using the coupling constants and chemical shifts given in the Experimental Section.

constant of 1350 Hz falls in the 100–9000 Hz range reported for other diplatinum compounds.³⁹

There is only one other example of a diplatinum(I) complex with six identical ligands. The hexakis(methylisonitrile)diplatinum(I) dication, $[\text{Pt}_2(\text{CNMe})_6]^{2+}$, has been prepared by reduction of potassium tetrachloroplatinate(II) with methylisonitrile in aqueous solution.⁴⁰

Reaction of $\text{Pt}(\text{PMe}_3)_4$ with $[\text{Pt}(\text{PMe}_3)_4][\text{hfac}]_2$: Isolation of the Platinum(II) Hydride $[\text{PtH}(\text{PMe}_3)_4][\text{hfac}]$, **3.** The unexpected platinum(II) hydride complex $[\text{PtH}(\text{PMe}_3)_4][\text{hfac}]$, **3**, is obtained when the reaction of equal molar quantities of $\text{Pt}(\text{PMe}_3)_4$ and $[\text{Pt}(\text{PMe}_3)_4][\text{hfac}]_2$ is carried out in tetrahydrofuran.



3

The clearest evidence for the identification of **3** as a hydride comes from its ^1H NMR and IR spectra. The ^1H NMR spectrum of **3** at room temperature features a signal at δ -13.37 that is coupled to the ^{195}Pt center with a $^1J_{\text{Pt-H}}$ coupling constant of 600 Hz. Both the chemical shift and the $^1J_{\text{Pt-H}}$ coupling constant are within the ranges observed for other known platinum(II) hydride complexes.^{41–48} No coupling to the ^{31}P nuclei is observed because dissociation of the phosphine ligands is fast at 25 °C (see below). The IR spectrum of **3** shows a

- (38) Krevor, J. V. Z.; Simonis, U.; Richter, J. A., II. *Inorg. Chem.* **1992**, *31*, 2409–2414.
- (39) Garth Kidd, R.; Goodfellow, R. J. In *NMR and the Periodic Table*; Harris, R. K., Mann, B. E., Eds.; Academic Press: New York, 1978; Table 8.27.
- (40) Boehm, J. R.; Doonan, D. J.; Balch, A. L. *J. Am. Chem. Soc.* **1976**, *98*, 4845–4850.
- (41) Roundhill, D. M. *Adv. Organomet. Chem.* **1975**, *13*, 273–361 and references therein.
- (42) English, A. D.; Meakin, P.; Jesson, J. P. *J. Am. Chem. Soc.* **1976**, *98*, 422–436.
- (43) Green, M.; Grove, D. M.; Spencer, J. L.; Stone, F. G. A. *J. Chem. Soc., Dalton Trans.* **1977**, 2228–2231.
- (44) Ellis, J. W.; Harrison, K. N.; Hoyer, P. A. T.; Orpen, A. G.; Pringle, P. G.; Smith, M. B. *Inorg. Chem.* **1992**, *31*, 3026–3033.
- (45) Brüggeller, P. *Inorg. Chem.* **1990**, *29*, 1742–1750.
- (46) Handler, A.; Peringer, P.; Müller, E. P. *J. Organomet. Chem.* **1991**, *412*, 451–456.
- (47) De Felice, V.; Ferrara, M. L.; Panunzi, A.; Ruffo, F. *J. Organomet. Chem.* **1992**, *439*, C49–C51.

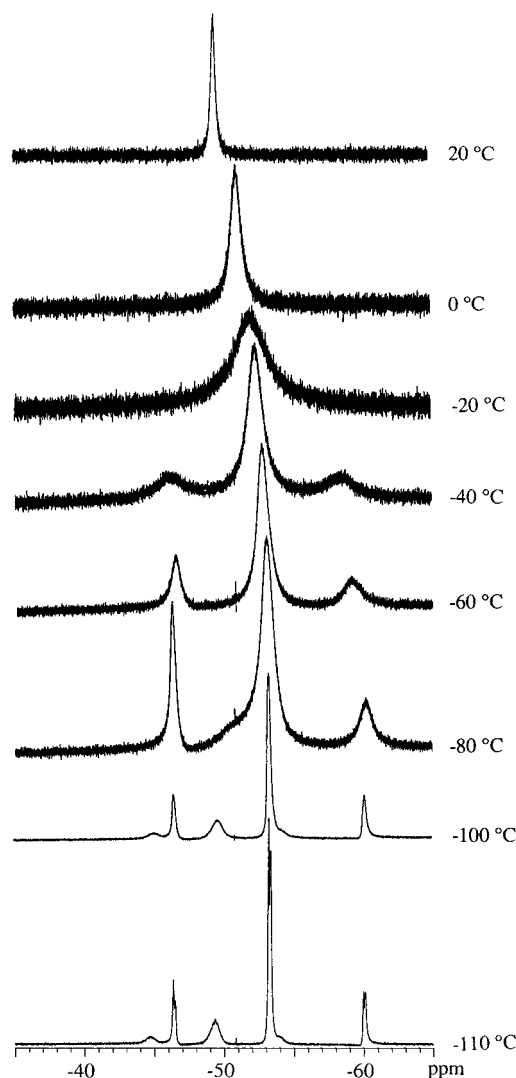
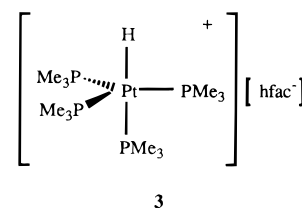


Figure 4. Variable-temperature 202 MHz $^{31}\text{P}\{^1\text{H}\}$ NMR spectra of $[\text{PtH}(\text{PMe}_3)_4][\text{hfac}]$, **3**, in a mixture of dimethyl ether and ethanol- d_6 .

characteristic Pt–H stretch at 2055 cm^{-1} . This frequency is consistent with the Pt–H stretching frequencies of other known platinum(II) hydride complexes.^{41–48}

The $^{31}\text{P}\{^1\text{H}\}$ NMR spectrum of **3** at -110 °C shows two sets of PMe_3 environments in an intensity ratio of 1:3 (Figure 4). These spectroscopic data are most consistent with a structure in which the platinum atom adopts a trigonal bipyramidal geometry with the hydride ligand occupying an axial position:



There are several examples of five-coordinate platinum(II) monohydride complexes. English *et al.* first observed that, in the presence of excess PEt_3 , the hydridotris(triethylphosphine)platinum(II) cation, $[\text{PtH}(\text{PEt}_3)_3][\text{BPh}_4]$, is in equilibrium with the hydridotetrakis(triethylphosphine)platinum(II) cation, $[\text{PtH}(\text{PEt}_3)_4][\text{BPh}_4]$, in CHClF_2 at very low temperatures (< -130

- (48) Cramer, R. D.; Lindsey, R. V.; Prewitt, C. T.; Stolberg, U. G. *J. Am. Chem. Soc.* **1965**, *87*, 658.

°C).⁴² Above -100 °C, only $[\text{PtH}(\text{PEt}_3)_3][\text{BPh}_4]$ is present in the solution. In contrast, the hydridotetrakis(phosphite)platinum(II) cations, $[\text{PtH}\{\text{P}(\text{OR})_3\}_4][\text{BPh}_4]$, where OR = OMe or OEt, are stable at room temperature.⁴³ The hydridotetrakis{tris-(hydroxymethyl)phosphine}platinum(II) cation, $[\text{PtH}\{\text{P}(\text{CH}_2\text{OH})_3\}_4][\text{OH}]$, is also stable in solution at room temperature.⁴⁴ With multidentate phosphines, stable hydridotetrakis(phosphine)platinum(II) cations can be isolated: among these are $[\text{PtH}(\text{p}_4)][\text{X}]$ (where p_4 is 1,1,4,7,10,10-hexaphenyl-1,4,7,10-tetraphosphadecane and X is BF_4 , BPh_4 , or AsF_6)⁴⁵ and $[\text{PtH}\{\text{PhP}(\text{CH}_2\text{CH}_2\text{PPh}_2)_2\text{L}\}[\text{O}_3\text{SCF}_3]$ (where L = PBu_3 , PPh_2H , PCy_2H , or $\eta^1\text{-Ph}_2\text{PCH}_2\text{PPh}_2$).⁴⁶ Also known are some related five-coordinate platinum(II) hydride complexes in which the phosphine ligands are replaced by other Lewis bases.^{47,48}

Of all the isolable five-coordinate platinum(II) hydride complexes mentioned above, only the tetraphenylborate salt of the $[\text{PtH}(\text{p}_4)^+]$ cation has been structurally characterized.⁴⁵ X-ray crystallography shows that it adopts a distorted trigonal-bipyramidal structure in the solid state with the hydride ligand occupying an axial site.⁴⁵

Since most of the five-coordinate platinum(II) hydride complexes discussed above are fluxional in solution, we should expect compound **3** also to be nonrigid in solution. Indeed, the ^1H NMR spectrum at 25 °C shows only one resonance at δ 1.60 instead of the two different PMe_3 environments expected.

Figure 4 shows the variable-temperature $^{31}\text{P}\{^1\text{H}\}$ NMR spectra of **3** in a mixture of dimethyl ether and ethanol- d_8 . The $^{31}\text{P}\{^1\text{H}\}$ NMR spectrum of **3** at -110 °C consists of two sets of peaks at δ -49.3 ($^1J_{\text{PtP}} = 1852$ Hz) and δ -53.4 ($^1J_{\text{PtP}} = 2763$ Hz) with relative intensities of 1:3. This spectrum also shows that the two phosphorus environments are coupled to each other with a $^2J_{\text{PP}}$ coupling constant of 30 Hz. When the temperature is increased to -100 °C, the $^{31}\text{P}\{^1\text{H}\}$ NMR spectrum still shows two sets of peaks, but the peaks are broader and the coupling between the two phosphorus environments is no longer discernible. At -40 °C the $^{31}\text{P}\{^1\text{H}\}$ NMR spectrum shows only a broad peak at δ -51.5 .

Trigonal bipyramidal complexes of stoichiometry $[\text{MH}(\text{PR}_3)_4]^{n+}$ are well-known to undergo several kinds of exchange processes. Some complexes are fluxional and the axial and equatorial phosphorus ligands exchange intramolecularly, probably via a mechanism known as the tetrahedral jump;^{49–51} other complexes exhibit fast intermolecular exchange involving dissociation of phosphine and formation of $[\text{MH}(\text{PR}_3)_3]^{n+}$. Notably, the phosphine ligand trans to the hydride is not permuted in this process.⁴² The variable-temperature spectra of **3** clearly indicate that exchange between the two phosphorus environments is occurring on the NMR time scale at -40 °C. Since the phosphorus resonance at -40 °C is still coupled to the ^{195}Pt center, the most logical explanation for this low-temperature exchange process is intramolecular PMe_3 exchange via a tetrahedral jump mechanism.^{42,49–51}

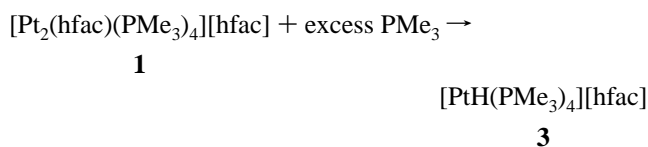
Above -40 °C, however, the coupling to the platinum nucleus is lost. This result strongly suggests that **3** undergoes a second dynamic process involving intermolecular exchange with free PMe_3 . The triethylphosphine analogue $[\text{PtH}(\text{PEt}_3)_4][\text{BPh}_4]$ is only stable at very low temperatures and dissociates to give the hydridotrakis(triethylphosphine)platinum(II) complex $[\text{PtH}(\text{PEt}_3)_3][\text{BPh}_4]$ above -100 °C;⁴² on the basis of this precedent,

we propose that **3** undergoes intermolecular exchange via a similar dissociative mechanism:



Consistent with this proposition, the $^{31}\text{P}\{^1\text{H}\}$ NMR chemical shift of **3** above -40 °C is temperature dependent and moves to higher frequency as the temperature is increased. This behavior can be explained by assuming that the concentrations of the hydridotrakis(trimethylphosphine)platinum cation and free PMe_3 increase at higher temperatures and that the phosphorus chemical shift of the tris(phosphine) complex $[\text{PtH}(\text{PMe}_3)_3][\text{hfac}]$ is deshielded relative to that of the tetrakis(phosphine) complex **3**.

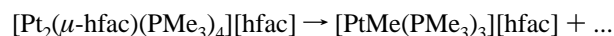
We have also been able to prepare compound **3** by addition of excess PMe_3 to a solution of the bridging hfac complex **1** in tetrahydrofuran.



In situ NMR experiments suggest that the hydride source in this reaction is adventitious water. When the reaction of **1** with PMe_3 is carried out in a septum-capped NMR tube in tetrahydrofuran- d_8 , the initial NMR spectrum contains no resonances ascribable to either $[\text{PtH}(\text{PMe}_3)_4][\text{hfac}]$ or $[\text{PtD}(\text{PMe}_3)_4][\text{hfac}]$. When the NMR tube is allowed to stand at 25 °C overnight, however, $[\text{PtH}(\text{PMe}_3)_4][\text{hfac}]$ forms and eventually becomes the only product observed in solution. The conversion proceeds more quickly by addition of small amounts of water to the NMR tube.

We have also prepared the tetraphenylborate salt of **3** via anion metathesis. The hfac anion in **3** can be replaced by stirring a mixture of **3** and NaBPh_4 in tetrahydrofuran at room temperature for 12 h, followed by recrystallization from a mixture of dichloromethane/diethyl ether.

Behavior of $[\text{Pt}_2(\mu\text{-hfac})(\text{PMe}_3)_4][\text{hfac}]$, **1, upon Thermolysis: Cleavage of Phosphorus–Carbon Bonds.** Due to its ionic nature, **1** is not appreciably volatile. Interestingly, however, when compound **1** is heated to 140 °C at 10^{-3} Torr in a sublimator, a light yellow, oily sublimate condenses on the cold finger. ^1H and $^{31}\text{P}\{^1\text{H}\}$ NMR spectroscopy shows that the sublimate is in fact a mixture of the platinum(II) methyl complex $[\text{PtMe}(\text{PMe}_3)_3][\text{hfac}]$ (50 mol %) and the platinum(II) trimethylphosphine complex $[\text{Pt}(\text{hfac})(\text{PMe}_3)_2][\text{hfac}]$ (50 mol %). The spectroscopic data for $[\text{PtMe}(\text{PMe}_3)_3][\text{hfac}]$ have been given in our previous paper,¹² and they are similar to those of the methylplatinum(II) cations $[\text{PtMeL}_3]^+$ (where L is PPh_3 or PMe_2Ph).^{52,53} This thermolysis result shows that platinum can activate the phosphorus–methyl bonds of PMe_3 ligands.



As discussed previously, cleavage of P–C bonds in unidentate trialkylphosphines is uncommon,¹² and the isolation of organometallic complexes resulting from the metal-promoted cleavage of phosphorus–alkyl bonds is even more unusual. The formation of palladium(II) methyl complex $[\text{PdMe}(\text{PMe}_3)_3][\text{hfac}]$ during thermolysis of $[\text{Pd}_2(\text{PMe}_3)_6][\text{hfac}]_2$ is the only other well-established example in which cleavage of a P–C

(49) Yoshida, T.; Thorn, D. L.; Okano, T.; Otsuka, S.; Ibers, J. A. *J. Am. Chem. Soc.* **1980**, *102*, 6451–6457.

(50) Meakin, P.; Muetterties, E. L.; Jesson, J. P. *J. Am. Chem. Soc.* **1972**, *94*, 5271–5285.

(51) Jesson, J. P.; Muetterties, E. L. In *Dynamic Nuclear Magnetic Resonance Spectroscopy*; Jackman, L. M., Cotton, F. A., Eds.; Academic Press: New York, 1975; Chapter 8.

(52) Clark, H. C.; Ruddick, J. D. *Inorg. Chem.* **1970**, *9*, 1226–1229.

(53) Peterson, J. L.; Nappier, Jr., T. E.; Meek, D. W. *J. Am. Chem. Soc.* **1973**, *95*, 8195–8197.

bond of an alkylphosphine leads to a product in which the alkyl group is retained.¹²

Our study of the chemistry of palladium PMe_3 compounds led us to predict that P–C bond cleavage could lead to incorporation of phosphorus and carbon impurities in films grown by chemical vapor deposition from precursors containing tertiary phosphine ligands,¹² and this prediction has recently been confirmed experimentally.⁵⁴ For $[\text{Pd}_2(\text{PMe}_3)_6][\text{hfac}]_2$, we suggested that the activation of P–C bonds occurs via disproportionation back to Pd^0 and Pd^{II} species and that the former are responsible for the activation chemistry. The existence of **1** (a Pt^0 – Pt^{II} mixed-valence species) and its ability to activate P–C bonds supports this suggestion.

Experimental Section

All operations were carried out under vacuum or under argon. Solvents were distilled under nitrogen from sodium benzophenone (pentane, diethyl ether, and tetrahydrofuran), magnesium (methanol), or calcium hydride (dichloromethane). Tetrahydrofuran- d_8 (Cambridge Isotopes) was dried by passage through a dehydrated alumina column inside a drybox. Sodium tetraphenylborate (Morton-Thiokol) was dried in a vacuum oven at 150 °C before use. Trimethylphosphine⁵⁵ and bis(hexafluoroacetylacetonato)platinum(II)⁵⁶ were prepared by following literature procedures.

Elemental analyses were performed by the University of Illinois Microanalytical Laboratory. The IR spectra were recorded on a Perkin-Elmer 599B instrument as Nujol mulls between KBr plates. The ^1H NMR data were recorded on a General Electric GN-500 spectrometer at 500 MHz, on a General Electric QE-300 spectrometer at 300 MHz, or on a General Electric GN-300NB spectrometer at 300 MHz; the ^{31}P NMR data were recorded on a General Electric GN-300NB spectrometer at 121 MHz. Chemical shifts are reported in δ units (positive shifts to high frequency) relative to TMS (^1H) or 85% H_3PO_4 (^{31}P). The simulation of the phosphorus line shape of complex **2** was carried out with the program NUTS available from AcornNMR. Melting points were determined on a Thomas–Hoover Unimelt apparatus in sealed capillaries under argon. Solution conductivities were measured at room temperature with a YSI Scientific Model 35 conductance meter and a glass dip cell with a cell constant of 1.0.

Tetrakis(trimethylphosphine)platinum(0), $\text{Pt}(\text{PMe}_3)_4$. To a solution of KOH (0.35 g, 6.25 mmol) and PMe_3 (1.5 mL, 14.8 mmol) in a mixture of EtOH (15 mL) and H_2O (1 mL) was added a solution of K_2PtCl_4 (0.75 g, 2.43 mmol) in H_2O (5 mL). A white precipitate formed initially which rapidly redissolved. The resulting colorless solution was stirred at 60 °C for 3 h to afford a pale yellow solution. The solvent was removed under vacuum, and the residue was extracted with pentane (3 \times 40 mL). The filtered extracts were combined and taken to dryness to yield a white powder. Yield: 0.40 g (44%). ^1H NMR (toluene- d_8 , 25 °C): δ 1.38 (s). $^{31}\text{P}\{^1\text{H}\}$ NMR (toluene- d_8 , 25 °C): δ –52.6 (s, $^1J_{\text{P-P}} = 3802$ Hz). These NMR spectroscopic data are essentially identical to those reported previously for $\text{Pt}(\text{PMe}_3)_4$.^{14,15}

(1,1,1,5,5,5-Hexafluoro-2,4-pentanedionato)bis(trimethylphosphine)platinum(II) 1,1,1,5,5,5-Hexafluoro-2,4-pentanedionate, $[\text{Pt}(\text{hfac})(\text{PMe}_3)_2][\text{hfac}]$. To a solution of $\text{Pt}(\text{hfac})_2$ (0.36 g, 0.59 mmol) in diethyl ether (30 mL) was added PMe_3 (0.12 mL, 1.19 mmol). The solution turned yellow instantly and was stirred at room temperature for 1 h. The yellow solution was filtered, concentrated to ca. 15 mL, and cooled to –20 °C to afford yellow crystals of the product. Yield: 0.34 g (75%). Mp: 122–126 °C. Anal. Calcd (found) for $\text{C}_{16}\text{H}_{20}\text{F}_6\text{O}_4\text{P}_2\text{Pt}$: C, 25.2 (25.4); H, 2.65 (2.64); P, 8.14 (8.08); Pt, 25.6 (25.5). Molar conductivity (nitrobenzene, 10^{-3} M): 30.0 Ω^{-1} cm^2 mol^{-1} . ^1H NMR (CD_2Cl_2 , 25 °C): δ 5.95 (br s, $\text{HC}(\text{CO}_2\text{CF}_3)_2$), 1.85 (d, $^2J_{\text{HP}} = 11.7$ Hz, PMe_3). $^{31}\text{P}\{^1\text{H}\}$ NMR (CD_2Cl_2 , 25 °C): δ –23.7 (s, $^1J_{\text{P-Pt}} = 3706$ Hz). IR (cm^{-1}): 1673 (s), 1637 (s), 1615 (m), 1558 (s), 1530 (m), 1432 (w), 1353 (vw), 1203 (m), 1260 (vs), 1228 (vs),

1178 (vs), 1153 (vs), 1123 (vs), 1065 (w), 975 (m), 953 (s), 934 (w), 870 (vw), 858 (vw), 808 (m), 782 (m), 748 (m), 683 (m), 660 (m), 595 (w), 574 (w).

Tetrakis(trimethylphosphine)platinum(II) 1,1,1,3,3,3-Hexafluoropentane-2,4-dionate, $[\text{Pt}(\text{PMe}_3)_4][\text{hfac}]_2$. To a solution of $\text{Pt}(\text{hfac})_2$ (0.29 g, 0.48 mmol) in diethyl ether (30 mL) was added PMe_3 (0.20 mL, 2.0 mmol). The solution immediately became colorless, and a white precipitate began to form. After the mixture had been stirred at room temperature for 1 h, the white precipitate was collected by filtration, washed with diethyl ether (5 mL), and dried under vacuum. Yield: 0.40 g (91%). Mp: 188–195 °C (dec). Anal. Calcd (found) for $\text{C}_{22}\text{H}_{38}\text{F}_6\text{O}_4\text{P}_4\text{Pt}$: C, 28.9 (28.8); H, 4.19 (4.22); P, 13.6 (13.3); Pt, 21.4 (21.1). ^1H NMR (CD_2Cl_2 , 25 °C): δ 5.52 (s, $\text{HC}(\text{CO}_2\text{CF}_3)_2$), 1.90 (s, PMe_3). $^{31}\text{P}\{^1\text{H}\}$ NMR (CD_2Cl_2 , 25 °C): δ –22.0 (s, $^1J_{\text{P-Pt}} = 2328$ Hz). IR (cm^{-1}): 1670 (vs), 1560 (vs), 1528 (s), 1512 (w), 1436 (w), 1317 (w), 1297 (w), 1246 (vs), 1176 (vs), 1148 (vs), 1116 (vs), 1062 (vw), 950 (vs), 861 (m), 797 (vw), 781 (m), 743 (vw), 734 (m), 673 (w), 668 (m), 573 (m).

(μ -1,1,1,5,5,5-Hexafluoro-2,4-pentanedionato)tetrakis(trimethylphosphine)diplatinum 1,1,1,5,5,5-Hexafluoro-2,4-pentanedionate, $[\text{Pt}_2(\mu\text{-hfac})(\text{PMe}_3)_4][\text{hfac}]$, **1.** To a slurry of $\text{Pt}(\text{hfac})_2$ (0.58 g, 0.95 mmol) in pentane (25 mL) was added a solution of $\text{Pt}(\text{PMe}_3)_4$ (0.48 g, 0.96 mmol) in pentane (10 mL). A red precipitate began to form immediately. After the mixture had been stirred for 1 h, the red precipitate was collected by filtration. Yield: 0.85 g (81% based on $\text{Pt}(\text{hfac})_2$). The crude product can be further purified by recrystallization from a mixture of CH_2Cl_2 (ca. 15 mL) and Et_2O (ca. 80 mL) at –78 °C to give orange crystals of the product. Mp: 132 °C (dec). Anal. Calcd (found) for $\text{C}_{22}\text{H}_{38}\text{F}_{12}\text{O}_4\text{P}_4\text{Pt}_2$: C, 23.8 (23.7); H, 3.46 (3.48); P, 11.2 (11.0); Pt, 35.2 (34.9). Molar conductivity (methanol, 10^{-3} M): 74.3 Ω^{-1} cm^2 mol^{-1} . ^1H NMR (C_6D_6 , 25 °C): δ 6.28 (s, 1 H, $\text{HC}(\text{COCF}_3)_2$), 4.29 (br s, $^2J_{\text{H-Pt}} = 39.0$ Hz, 1 H, $\text{Pt}-\text{CH}(\text{COCF}_3)_2$), 1.22 (d, $^2J_{\text{HP}} = 10.2$ Hz, $^3J_{\text{H-Pt}} = 19.2$ Hz, 18 H, PMe_3), 1.18 (“t”, $^2J_{\text{HP}} + ^4J_{\text{HP}} = 10.7$ Hz, 18 H, PMe_3). $^{31}\text{P}\{^1\text{H}\}$ NMR (C_6D_6 , 25 °C): δ –22.3 (s, $^1J_{\text{P-Pt}} = 3980$ Hz), –27.0 (s, $^2J_{\text{P-Pt}} = 3636$ Hz). IR (cm^{-1}): 1670 (vs), 1555 (s), 1524 (s), 1429 (m), 1318 (w), 1299 (w), 1295 (w), 1252 (vs), 1182 (vs), 1147 (vs), 1120 (s), 1018 (m), 946 (vs), 885 (s), 858 (w), 820 (m), 779 (w), 731 (s), 673 (m), 654 (m), 600 (w), 572 (w), 533 (vw).

Hexakis(trimethylphosphine)diplatinum(I) 1,1,1,5,5,5-Hexafluoro-2,4-pentanedionate, $[\text{Pt}_2(\text{PMe}_3)_6][\text{hfac}]_2$, **2.** To a solution of $[\text{Pt}(\text{hfac})(\text{PMe}_3)_2][\text{hfac}]$ (0.21 g, 0.24 mmol) in diethyl ether (20 mL) was added a solution of $\text{Pt}(\text{PMe}_3)_4$ (0.14 g, 0.28 mmol) in diethyl ether (5 mL) at room temperature. The resulting colorless solution was stirred at room temperature for 12 h to afford the product as a white precipitate. Yield: 0.14 g (46%). Anal. Calcd (found) for $\text{C}_{28}\text{H}_{56}\text{F}_{12}\text{O}_6\text{P}_6\text{Pt}_2$: C, 26.7 (27.6); H, 3.48 (5.07); P, 14.7 (15.2). The crude product can be further purified by recrystallization from a mixture of dichloromethane and diethyl ether. ^1H NMR (CD_2Cl_2 , 25 °C): δ 5.45 (s, 2 H, $\text{HC}(\text{COCF}_3)_2$), 1.79 (“t”, $^2J_{\text{H-Pt}} + ^4J_{\text{H-Pt}} = 5.5$ Hz, $^2J_{\text{Pt-H}} = 29.5$ Hz, 36 H, PMe_3), 1.18 (m, $^2J_{\text{P-H}} = 29.0$ Hz, 18 H, PMe_3). The $^{31}\text{P}\{^1\text{H}\}$ NMR spectrum in CD_2Cl_2 at 25 °C can be simulated as a superposition of $\text{AA}'\text{B}_2\text{B}'_2$, $\text{ABC}_2\text{D}_2\text{M}$, and $\text{AA}'\text{B}_2\text{B}'_2\text{MM}'$ spin systems depending on the number of ^{195}Pt nuclei present. For the $\text{AA}'\text{B}_2\text{B}'_2$ spin system, the parameters were $\delta_{\text{A}} = -21.9$, $\delta_{\text{B}} = -26.9$, $^2J_{\text{AB}} = 21.8$ Hz, $^3J_{\text{AA}'} = 161.0$ Hz, $^3J_{\text{AB}'} = 4.8$ Hz, and $^3J_{\text{BB}'} = 0$ Hz. The platinum satellites gave the following couplings: $^1J_{\text{A-Pt}} = 2079$ Hz, $^1J_{\text{B-Pt}} = 2656$ Hz, $^2J_{\text{A-Pt}} = 414$ Hz, $^2J_{\text{B-Pt}} = -122$ Hz, and $^1J_{\text{Pt-Pt}} = 1350$ Hz. Many of the features in the $\text{AA}'\text{B}_2\text{B}'_2\text{MM}'$ spectrum due to the doubly ^{195}Pt -labeled isotopolog were insensitive to the magnitude of $^1J_{\text{Pt-Pt}}$. This coupling constant was established from the positions of small features near δ –20, –34, and –36.5. IR (cm^{-1}): 1670(s), 1550 (m), 1292 (m), 1210 (m), 1170 (vs, br), 1125 (vs), 1090 (s), 942 (vs), 854 (s), 795 (s), 720 (s), 666 (m), 656 (m).

Hydridotetrakis(trimethylphosphine)platinum(II) 1,1,1,5,5,5-Hexafluoro-2,4-pentanedionate, $[\text{PtH}(\text{PMe}_3)_4][\text{hfac}]$, **3.** To a mixture of $\text{Pt}(\text{PMe}_3)_4$ (0.13 g, 0.26 mmol) and $[\text{Pt}(\text{PMe}_3)_4][\text{hfac}]_2$ (0.20 g, 0.22 mmol) was added tetrahydrofuran (25 mL) at room temperature. The resulting solution was stirred at room temperature for 12 h to afford a light yellow solution. The solvent was removed under vacuum, and the residue was extracted into CH_2Cl_2 (15 mL). The yellow CH_2Cl_2 solution was concentrated to ca. 5 mL, and diethyl ether (ca. 10 mL)

(54) Yuan, Z.; Jiang, D.; Naftel, S. J.; Sham, T.-K.; Puddephatt, R. J. *Chem. Mater.* **1994**, *6*, 2151–2158.

(55) Luetkens, M. L.; Sattelberger, A. P.; Murray, H. H.; Basil, J. D.; Fackler, J. P. *Inorg. Synth.* **1989**, *26*, 7–12.

(56) Okeya, S.; Kawaguchi, S. *Inorg. Synth.* **1980**, *20*, 65–69.

was added. The solution was then cooled to $-20\text{ }^{\circ}\text{C}$ to afford colorless microcrystals of the product. Yield: 0.15 g (48%). Mp: 161–165 $^{\circ}\text{C}$ (dec). Anal. Calcd (found) for $\text{C}_{17}\text{H}_{38}\text{F}_6\text{O}_2\text{P}_4\text{Pt}$: C, 28.9 (29.1); H, 5.41 (5.46); P, 17.5 (15.9); Pt, 27.6 (27.0). Molar conductivity (methanol, 10^{-3} M): $82\ \Omega^{-1}\text{ cm}^2\text{ mol}^{-1}$. $^1\text{H NMR}$ (CD_2Cl_2 , $25\text{ }^{\circ}\text{C}$): δ 5.41 (br s, 1 H, $\text{HC}(\text{COCF}_3)_2$), 1.60 (d, $^2J_{\text{P-H}} = 8.4\text{ Hz}$, 36 H, PMe_3), -13.37 (s, $^1J_{\text{Pt-H}} = 600\text{ Hz}$, 1 H, Pt-H). $^{31}\text{P}\{^1\text{H}\}$ NMR (CD_2Cl_2 , $0\text{ }^{\circ}\text{C}$): δ -51.2 (br s). $^{31}\text{P}\{^1\text{H}\}$ NMR (CD_2Cl_2 , $-110\text{ }^{\circ}\text{C}$): δ -49.3 (t, $^2J_{\text{PP}} = 30\text{ Hz}$, $^1J_{\text{Pt-P}} = 1906\text{ Hz}$, 1 P, axial PMe_3), -53.4 (t, $^2J_{\text{PP}} = 30\text{ Hz}$, $^1J_{\text{Pt-P}} = 2741\text{ Hz}$, 3 P, equatorial PMe_3). IR (cm^{-1}): 2055 (s), 1670 (s), 1562 (vs), 1524 (s), 1508 (w), 1427 (m), 1309 (m), 1290 (m), 1241 (s), 1150 (vs, vbr), 1065 (w), 944 (vs), 850 (s), 730 (s), 675 (s), 657 (s), 572 (s), 522 (w).

Hydridotetrakis(trimethylphosphine)platinum(II) Tetraphenylborate, $[\text{PtH}(\text{PMe}_3)_4][\text{BPh}_4]$, **3'.** To a solution of **1** (0.20g, 0.18 mmol) in tetrahydrofuran (40 mL) was added PMe_3 (0.1 mL, 1.0 mmol) at room temperature. The solution turned colorless immediately and was then transferred to a round bottom flask charged with NaBPh_4 (0.135 g, 0.43 mmol). After being stirred at room temperature for 12 h, the cloudy suspension was filtered to afford a colorless solution. The solvent was removed under vacuum, and the residue was extracted into CH_2Cl_2 (10 mL). The pale yellow CH_2Cl_2 extract was filtered, and to the filtrate was added diethyl ether (ca. 10 mL). The solution was then cooled to $-20\text{ }^{\circ}\text{C}$ to afford colorless microcrystals of the product. Yield: 0.18 g (61%). Anal. Calcd (found) for $\text{C}_{36}\text{H}_{57}\text{BP}_4\text{Pt}$: C, 52.7 (51.4); H, 7.01 (6.99); P, 15.1 (13.8); Pt, 23.8 (20.8). $^1\text{H NMR}$ (CD_2Cl_2 , $25\text{ }^{\circ}\text{C}$): δ 7.32 (br m, 8 H, $o\text{-C}_6\text{H}_5$), 7.03 (t, $^3J_{\text{HH}} = 7.5\text{ Hz}$, 8 H, $m\text{-C}_6\text{H}_5$), 6.88 (t, $^3J_{\text{HH}} = 7.5\text{ Hz}$, 8 H, $p\text{-C}_6\text{H}_5$), 1.57 (d, $^2J_{\text{PH}} = 8.0\text{ Hz}$, 36 H, PMe_3), -13.40 (s, $^1J_{\text{Pt-H}} = 600\text{ Hz}$, 1 H, Pt-H). $^{31}\text{P}\{^1\text{H}\}$ NMR (CD_2Cl_2 , $0\text{ }^{\circ}\text{C}$): δ -51.0 (br s). IR (cm^{-1}): 3028 (s), 2044 (s), 1944 (vw), 1882 (vw), 1810 (vw), 1675 (m), 1582 (m), 1534 (m), 1478 (m), 1422 (s), 1303 (m), 1286 (s), 1258 (s), 1204 (m), 1153 (s), 1133 (m), 1079 (vw), 1064 (vw), 1030 (w), 942 (vs), 854 (s), 846 (s), 790 (w), 740 (s), 730 (s), 703 (s), 670 (s), 617 (w), 622 (w), 610 (w), 602 (m), 580 (vw), 478 (vw), 462 (vw).

Thermolysis of $[\text{Pt}_2(\mu\text{-hfac})(\text{PMe}_3)_4][\text{hfac}]$ and Identification of Methyltris(trimethylphosphine)platinum(II) 1,1,1,5,5,5-Hexafluoro-2,4-pentanedionate, $[\text{PtMe}(\text{PMe}_3)_3][\text{hfac}]$, **4.** A sample of $[\text{Pt}_2(\mu\text{-hfac})(\text{PMe}_3)_4][\text{hfac}]$ (0.20 g, 0.18 mmol) was placed in a sublimator equipped with a cold finger; the latter was cooled to $-78\text{ }^{\circ}\text{C}$. The sublimator was evacuated and heated to $140\text{ }^{\circ}\text{C}$ for ca. 1.5 h. A dark involatile residue (ca. 0.1 g) remained after the sublimation was complete. The yellow oily sublimate was collected and examined by NMR spectroscopy. The spectrum contained the following resonances due to the platinum(II) complex $[\text{PtMe}(\text{PMe}_3)_3][\text{hfac}]$: $^1\text{H NMR}$ (CD_2Cl_2 , $-80\text{ }^{\circ}\text{C}$): δ 5.60 (s, $\text{HC}(\text{COCF}_3)_2$), 1.50 (br s, PMe_3), 0.23 (dt, $^3J_{\text{HP}(\text{cis})} = 8.2\text{ Hz}$, $^3J_{\text{HP}(\text{trans})} = 6.5\text{ Hz}$, $^2J_{\text{H-Pt}} = 57\text{ Hz}$, Pt-Me); $^{31}\text{P}\{^1\text{H}\}$ NMR (CD_2Cl_2 , $-80\text{ }^{\circ}\text{C}$) δ -17.9 (d, $^2J_{\text{PP}} = 24.0\text{ Hz}$, $^1J_{\text{P-Pt}} = 2558\text{ Hz}$), -24.1 (t, $^2J_{\text{PP}} = 24.0\text{ Hz}$, $^1J_{\text{P-Pt}} = 1803\text{ Hz}$). Also present in the sublimate in about 50 mol % is the platinum(II) complex $[\text{Pt}(\text{hfac})(\text{PMe}_3)_2][\text{hfac}]$.

Crystallographic Studies.⁵⁷ Single crystals of $[\text{Pt}_2(\mu\text{-hfac})(\text{PMe}_3)_4][\text{hfac}]$, **1**, grown from tetrahydrofuran, were mounted on glass fibers with Paratone-N oil (Exxon) and immediately cooled to $-75\text{ }^{\circ}\text{C}$ in a cold nitrogen gas stream on the diffractometer. Standard peak search

and indexing procedures gave rough cell dimensions, and the diffraction symmetry was confirmed by inspection of the axial photographs. Least-squares refinement using 25 reflections yielded the cell dimensions given in Table 1.

Data were collected in two quadrants of reciprocal space ($-h, \pm k, \pm l$) by using the measurement parameters listed in Table 1. The triclinic cell was consistent with space groups $P1$ and $P\bar{1}$. The average values of the normalized structure factors suggested the centric choice $P\bar{1}$, which was confirmed by successful refinement of the proposed model. The measured intensities were reduced to structure factor amplitudes and their esd's by correction for background, scan speed, Lorentz, and polarization effects. While corrections for crystal decay were unnecessary, absorption corrections were applied, the maximum and minimum transmission factors being 0.629 and 0.398. Seven questionable reflections with asymmetric peaks were deleted. Symmetry-equivalent reflections were averaged to yield the set of unique data. Only those data with $I > 2.58\sigma(I)$ were used in the least-squares refinement.

The structure was solved using direct methods (SHELXS-86) using Patterson and weighted difference Fourier methods. The correct positions for the platinum atoms were deduced from a vector map. Subsequent least-squares refinement and difference Fourier calculations revealed the positions of the remaining non-hydrogen atoms. The hydrogen atoms were included as fixed contributors in "idealized" positions with $\text{C-H} = 0.96\text{ \AA}$ (H3 never surfaced and was not included in the structure factor calculations). The quantity minimized by the least-squares program was $\sum w(|F_o| - |F_c|)^2$, where $w = 2.39/(\sigma(F_o)^2 + pF_o^2)$. The analytical approximations to the scattering factors were used, and all structure factors were corrected for both real and imaginary components of anomalous dispersion. In the final cycle of least squares, anisotropic thermal coefficients were refined for the non-hydrogen atoms, an independent isotropic thermal parameter was refined for H8, and a common group isotropic thermal parameter was refined for the remaining hydrogen atoms. An empirical isotropic extinction parameter was refined to a final value of $4.6(5) \times 10^{-8}$. Successful convergence was indicated by the maximum shift/error of 0.003 for the last cycle. Final refinement parameters are given in Table 1. The largest peaks in the final difference Fourier difference map (1.24 e \AA^{-3}) were located in the vicinity of the platinum atoms. A final analysis of variance between observed and calculated structure factors showed a slight dependence on $\sin \theta$.

Acknowledgment. We thank the Department of Energy (Grant DEFG02-91ER45439) for support of this work and Teresa Prussak-Wieckowska for assistance with the X-ray crystal structure determination. W.L. thanks the Department of Chemistry at the University of Illinois for a fellowship.

Supporting Information Available: Tables of full crystal data, atomic coordinates, calculated hydrogen atom positions, anisotropic thermal parameters, and complete bond distances and angles for $[\text{Pt}_2(\mu\text{-hfac})(\text{PMe}_3)_4][\text{hfac}]$; an ORTEP diagram of the hfac anion, and figures of the ^1H and $^{31}\text{P}\{^1\text{H}\}$ NMR spectra of $[\text{Pt}_2(\mu\text{-hfac})(\text{PMe}_3)_4][\text{hfac}]$ and of the variable-temperature ^1H NMR spectrum of $[\text{PtH}(\text{PMe}_3)_4][\text{hfac}]$ (11 pages). Ordering information is given on any current masthead page.

(57) For full details of the crystallographic methods and programs employed, see: Jensen, J. A.; Wilson, S. R.; Girolami, G. S. *J. Am. Chem. Soc.* **1988**, *110*, 4977–4982.